


# Numerical 2D MHD simulations of the collapse of magnetic rotating protostellar clouds with the Enlil code

Sergey Khaibrakhmanov<sup>1,2</sup> , Sergey Zamozdra<sup>2</sup>,  
Natalya Kargaltseva<sup>1,2</sup>, Andrey Zhilkin<sup>3</sup> and Alexander Dudorov<sup>2†</sup>

<sup>1</sup>Ural Federal University, 51 Lenina str., Ekaterinburg, 620000, Russia  
email: [khaibrakhmanov@csu.ru](mailto:khaibrakhmanov@csu.ru)

<sup>2</sup>Chelyabinsk State University, 129 Br. Kashirinykh str., Chelyabinsk, 454001, Russia

<sup>3</sup>Institute of Astronomy of the Russian Academy of Sciences (INASAN), Moscow, 119017, Russia

**Abstract.** We numerically investigate the gravitational collapse of rotating magnetic protostellar clouds. The simulations are performed using 2D MHD code ‘Enlil’. The code is based on TVD scheme of increased order of accuracy. We developed a model of the initially non-uniform cloud, which self-consistently treats gas density and large-scale magnetic field distribution. Simulation results for the typical parameters of a solar mass cloud are presented. In agreement with our previous results for the uniform cloud, the isothermal collapse of the non-uniform cloud results in formation of hierarchical structure of the cloud, consisting of flattened envelope and thin quasi-magnetostatic primary disk near its equatorial plane. The non-uniform cloud collapses longer than the uniform one, since the magnetic field is dynamically stronger at the periphery of the cloud in the former case.

**Keywords.** magnetic fields, magnetohydrodynamics (MHD), numerical simulation, star formation, interstellar medium

---

## 1. Introduction

Contemporary star formation takes place in gravitationally bound cores of molecular clouds, which are called protostellar clouds (PSCs hereafter) or prestellar cores. PSCs rotate with typical ratio of the rotational energy to the gravitational energy of few percents (Goodman et al. 1993; Caselli et al. 2002). Large-scale magnetic field is ubiquitous in the PSCs with typical magnetic field strength of  $10^{-5} - 10^{-4}$  G and non-dimensional mass-to-flux ratio of 2–3 (Li et al. 2009; Crutcher 2012).

The first numerical simulations of the gravitational collapse of PSCs have shown that electromagnetic and centrifugal forces cause the flattening of the cloud along the rotation axis and magnetic field direction and further formation of disks around protostars during the collapse (Nakano 1979; Black & Scott 1982; Dorfi 1982). This result has been confirmed by numerous simulations later on (see, e.g., Dudorov et al. 1999b, 2000; Zhao et al. 2020).

Modern observations have revealed large flattened envelopes around very young protostars in so-called class 0 young stellar objects. High-angular resolution observations with The Atacama Large Millimeter/Submillimeter Array (ALMA) indicate to the presence

<sup>†</sup>Professor Alexander Dudorov has passed away.

**Table 1.** Models of initial non-uniform large-scale magnetic field in PSCs.

N	Approach	References
1	Magneto-hydrostatic equilibrium	Stodólkiewicz (1963), Mouschovias (1976), Tomisaka <i>et al.</i> (1988), Carry & Stahler (2001), Allen <i>et al.</i> (2003)
2	Relaxation to magneto-hydrostatic equilibrium	Habe <i>et al.</i> (1991), Leao <i>et al.</i> (2013)
3	Straight magnetic lines with prescribed ratio of gas and magnetic pressures $P/P_m$	Mouschovias & Morton (1991), Banerjee & Pudritz (2006)
4	Straight magnetic lines with $B \propto N$ (column density)	Hennebelle & Ciardi (2009)
5	Straight magnetic lines with prescribed radial profile $B(R)$	Seifried <i>et al.</i> (2012), Myers <i>et al.</i> (2013)
6	Straight magnetic lines with constant mass-to-flux ratio	Gray <i>et al.</i> (2018)
7	Curved magnetic lines with prescribed vector potential $A_\phi(R)$	Tsukamoto <i>et al.</i> (2020)

of small possibly keplerian disks around protostars inside those flattened envelopes (see, e.g., Tobin *et al.* 2020). It is of great interest to study the conditions for the formation of rotationally supported protostellar disks (RSD), since they further evolve into accretion disks, which ultimately become protoplanetary disks of young stars. The main problem in this field is so-called magnetic braking catastrophe, i. e. too efficient transport of the cloud/disk angular momentum preventing the formation of RSD (see recent review Zhao *et al.* 2020). In order to tackle this problem, it is important to simulate initial stages of the cloud's collapse taking into account dissipative magneto-gas-dynamics (MHD) effects.

One of the problem in the simulations of the collapse of PSCs is a choice of the initial conditions. According to observations (see review in Gomez *et al.* 2021), PSCs have non-uniform density distribution. Usually, the radial profile of the cloud's density is approximated by power-law functions, although power-law indexes may vary in a wide range. Large-scale magnetic field of PSCs is also non-uniform. Typically PSCs have magnetic field with hour-glass geometry (Li *et al.* 2009), which is in agreement with theoretical predictions (Dudorov & Zhilkin 2008).

In Table 1, we summarize theoretical approaches used to set initial non-uniform large-scale magnetic field in the simulations of the PSC's collapse. Solution of the magneto-hydrostatic equilibrium equations (N1) is the difficult problem, therefore the problem of cloud's relaxation to the magneto-hydrostatic equilibrium can be considered (N2). The approaches (N3–N6) are more simple: straight magnetic lines with prescribed intensity. The straight lines guarantee a divergence free magnetic field. The approach N7 admits curved magnetic lines. All the approaches N3–N7 give more realistic field than the uniform field, but remain non-physical one.

In our previous works, we investigated the isothermal collapse of initially uniform magnetic rotating PSC (Khaibrakhmanov *et al.* 2021; Kargaltseva *et al.* 2021). We analyzed the hierarchical structure of the collapsing cloud, consisting of a flattened envelope, which contains quasi-magnetostatic primary disk (PD) inside with the first hydrostatic core in its center. The simulations have shown that the fast shock MHD wave moves outward from the PD boundary into the envelope, and a region of magnetic braking is formed behind the wave front. The PD play a key role in the evolution of the angular momentum of the system. In this work, we further develop our model and propose new self-consistent approach to model the initial state of the PSC with non-uniform magnetic field. The collapse of such a non-uniform PSC with typical parameters is numerically simulated and compared with our results for the uniform PSC.

## 2. Problem statement

We model the collapse of non-uniform spherical rotating cloud with non-uniform magnetic field. The density distribution is Plummer-like (Whitworth & Ward-Thompson 2001):

$$\rho = \frac{\rho_c}{1 + (r/r_1)^2}, \tag{2.1}$$

where  $\rho_c$  is the central density,  $r_1 = \pi^{-1/2}(M_0/\rho_c)^{1/3}$  is the characteristic radius of the cloud’s dense part,  $M_0$  is the mass of the cloud. The function (2.1) has the asymptotic power-law index  $-2$  that fits the PSC observations (Gomez et al. 2021).

The initial magnetic field is poloidal. It is calculated under the assumption of the PSC formation via spherically symmetric contraction of uniform medium with density  $\rho_0$  penetrated by uniform magnetic field  $\mathbf{B}_0$ . If the magnetic field is frozen into gas then  $\mathbf{B} \propto \rho \delta \mathbf{l}$ , where  $\delta \mathbf{l}$  is the length element. In spherical coordinates  $(r, \theta, \phi)$

$$\delta l_r \propto dR, \quad \delta l_\theta \propto R, \tag{2.2}$$

where  $R$  is the radius of spherical layer,  $dR$  is the width of the layer. Since the mass of the layer  $dm = 4\pi\rho R^2 dR$  is conserved then relations (2.2) yields

$$B_r \propto R^{-2}, \quad B_\theta \propto \rho R. \tag{2.3}$$

Let  $\rho = \rho_c f(r)$ . The mass of the matter inside a sphere with initial radius  $R_i$  is conserved, therefore

$$\rho_c V_\star = \rho_0 R_i^3 / 3, \quad V_\star \equiv \int_0^R f(r) r^2 dr. \tag{2.4}$$

Let’s express  $R_i$  from eq. (2.4) and substitute into relations (2.3) to obtain the law of frozen magnetic field evolution during the cloud formation

$$\frac{B_r}{B_{r0}} = R^{-2} \left( 3V_\star \frac{\rho_c}{\rho_0} \right)^{2/3}, \quad \frac{B_\theta}{B_{\theta0}} = R f(R) \left( \frac{\rho_c}{\rho_0} \right)^{2/3} (3V_\star)^{-1/3}. \tag{2.5}$$

In the case of uniform contraction  $f(r) = 1$  and  $V_\star = R^3/3$ , so the law (2.5) yields  $B_r, B_\theta \propto \rho^{2/3}$  as expected.

The collapse of the cloud is investigated using the equations of gravitational MHD. Numerical modeling is performed with the help of the 2D numerical code ‘Enlil’ based on the TVD scheme of the increased order of accuracy (Dudorov et al. 1999a,b; Zhilkin et al. 2009). Thermal evolution of the cloud is simulated using the equation of state with variable adiabatic index (see Kargaltseva et al. 2021).

## 3. Results

In this section we compare two simulations of initially uniform (run I) and non-uniform cloud (run II). We consider the PSC with mass of  $M_0 = 1 M_\odot$  and temperature of 10 K. Uniform cloud has density  $\rho_c = 1.5 \cdot 10^{-18}$  g cm $^{-3}$  and radius  $R_0 = 0.022$  pc. Non-uniform cloud has central density  $\rho_c = 3.5 \cdot 10^{-18}$  g cm $^{-3}$ , radius  $R_0 = 0.021$  pc and characteristic radius  $r_1 = 0.015$  pc. The ratios of thermal, rotation and magnetic energies of the cloud to the modulus of its gravitational energy are  $\varepsilon_t = 0.3$ ,  $\varepsilon_m = 0.2$ ,  $\varepsilon_w = 0.01$ , respectively.

In Figure 1, we show the structure of the clouds in runs I and II at the onset of the collapse (left panels), and at the moment of the first hydrostatic core formation (right panels).

Our simulations show that the general picture of the collapse in run II is similar to that in run I. In both cases, the cloud acquires a hierarchical structure at the end of

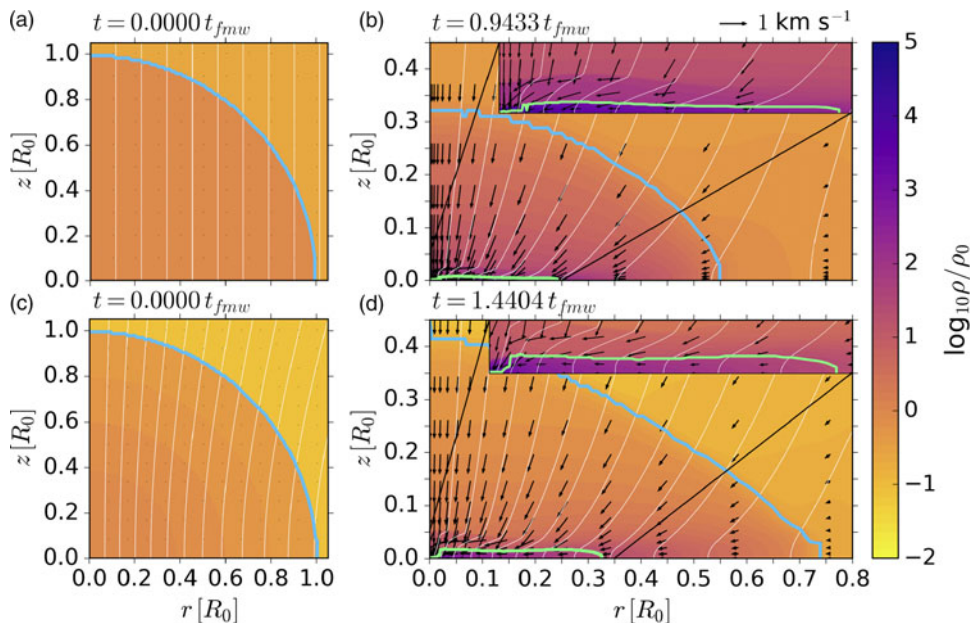


**Figure 1.** Two-dimensional structure of collapsing PSCs with initially uniform (upper panels) and non-uniform (lower panels) distributions of density and magnetic field. Left panels: initial state, right panels: moment of the first hydrostatic core formation. Initial parameters of the clouds:  $\varepsilon_t = 0.3$ ,  $\varepsilon_m = 0.2$ ,  $\varepsilon_w = 0.01$ . A quarter of the cloud in the region of positive  $r$  and  $z$  is considered. Color filling shows logarithm of non-dimensional density, arrows show the velocity field, and white lines are the poloidal magnetic field lines. The green line shows the border of the PD, the blue line is the boundary of the cloud. Insets in the upper right corners of panels (b) and (d) show the zoomed-in region near the primary disk.

the isothermal collapse. The hierarchy consists of a flattened envelope with thin quasi-magnetostatic PD near its equatorial plane. Further the first core forms in the center of the PD.

Figure 1(d) shows that flattened envelope has radius  $R \approx 0.75 R_0$  and half-thickness  $Z \approx 0.4 R_0$ , while the PD is characterized by  $R \approx 0.35 R_0$  and half-thickness  $Z \approx 0.02 R_0$ . These characteristics are larger than in run I, according to Figures 1(b) and (d). The degrees of flattening of each structure,  $Z/R$ , are similar in both runs:  $Z/R \approx 0.6$  for the envelope and  $Z/R \approx 0.04 - 0.06$  for the PD.

The main difference between runs I and II is that initially non-uniform cloud evolves slower. The first core forms at  $t = 1.44 t_{\text{fmw}}$  in run II, while it happens at  $t = 0.94 t_{\text{fmw}}$  in run I. Here  $t_{\text{fmw}}$  is the typical dynamical time of the collapse taking into account the effects of rotation and magnetic field (Dudorov & Sazonov (1982), see also Khaibrakhmanov *et al.* (2021)). This is explained by the fact that initial magnetic field is dynamically stronger at the periphery of the cloud in run II as compared to run I.

In order to describe the hierarchical structure of the cloud in run II, we plot density profiles  $\rho(r, 0)$  and  $\rho(0, z)$ , as well as vertical velocity profiles at several radii in Figure 2. Figure 2(a) clearly demonstrates the flattening of the cloud. There are three pronounced density jumps in the vertical density profile. Analysis of this dependence together with the velocity profile at  $r = 0.05 R_0$  shows that the first jump at  $z \approx 0.02 R_0 \approx 70$  au corresponds to the surface of the quasi-magnetostatic ( $v_z \rightarrow 0$ ) PD. The second jump,  $z \approx 0.05 R_0 \approx 200$  au, lies at the front of fast MHD shock wave propagating from the PD into the envelope. The third jump at  $z \approx 0.5 R_0 \approx 2000$  au is the contact boundary of the cloud.

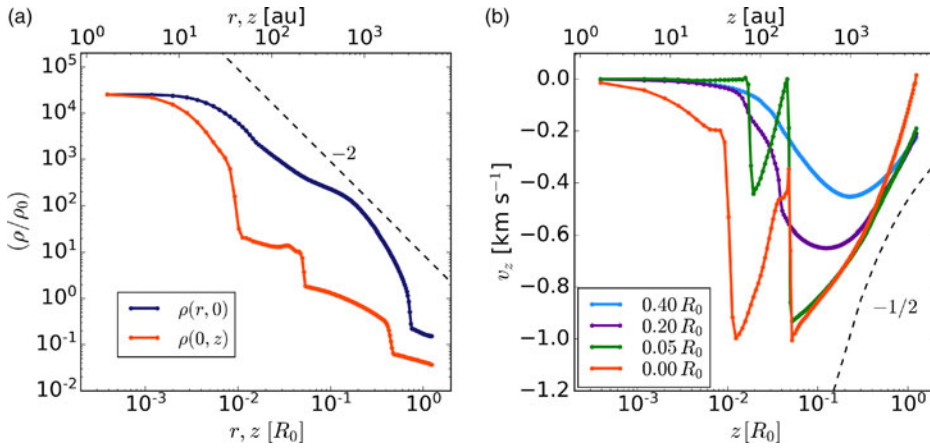


**Figure 2.** Panel (a): the profiles of gas density along the equatorial plane of the cloud (blue line) and along the rotation axis (orange line) in run II. Moment of time corresponds to Figure 1(d). Panel (b): corresponding profiles of vertical velocity  $v_z$  along the rotation axis at  $r = 0$  (orange line),  $r = 0.05 R_0$  (green line),  $r = 0.2 R_0$  (purple line) and  $r = 0.4 R_0$  (blue line). Dashed lines with labels show typical slopes.

Analogous jumps are seen in profiles  $v_z(z)$  at  $r = 0$  and  $r = 0.2 R_0$ . At further distances,  $r > 0.2 R_0$ , the quasi-magnetostatic equilibrium is not established.

Figures 1(d) and 2(b) show that the half-thickness of the primary disk is minimal,  $Z_{\min} \approx 40$  au, near the rotation axis,  $r = 0$ . Ten computational cells fit into the primary disk in this region, and maximum cell size  $\Delta z$  is of 3 au, i.e.  $\Delta z \ll Z_{\min}$ . At further radii  $r$ , number of cells that fit into the primary disk is even more. This means that the adopted grid resolution is sufficient to resolve the internal structure of the primary disk.

#### 4. Conclusions and discussion

In this work, we presented a numerical MHD model of the collapse of initially non-uniform PSC. Distinctive feature of the model is self-consistent treatment of both initial density and large-scale magnetic field distribution in the cloud. Initial density profile has the asymptotic power-law index  $-2$  that fits the PSC observations. Initial magnetic field distribution is determined considering that the cloud forms as a result of spherically symmetric contraction under condition of frozen-in magnetic field.

Numerical simulation of the collapse of such a non-uniform PSC of solar mass under typical parameters show that general picture of the collapse is similar to that of the initially uniform magnetic field. The cloud acquires a hierarchical structure during the isothermal collapse, consisting of flattened envelope and thin quasi-magnetostatic PD near its equatorial plane. The main difference between initially uniform and non-uniform clouds is that the isothermal collapse lasts longer in the latter case. This is explained by the following. For a fixed total magnetic energy of the cloud, the magnetic field is dynamically stronger at the periphery of non-uniform cloud, since the gas pressure in this case is smaller than in the case of uniform cloud, while the magnetic pressures are nearly the same.

In future, we plan to apply the developed model to study angular momentum and magnetic flux evolution of PSCs for various initial parameters in order to investigate efficiency of magnetic braking at the initial stages of the collapse. Results of the simulations will be used to construct synthetic maps of collapsing PSCs in sub-mm range and to investigate observational appearance of PD.

## Acknowledgments

This work is supported by the Russian Science Foundation, project 19-72-10012. The authors thank anonymous referee for useful comments.

## References

- Allen, A., Li, Z.-Y., & Shu, F. H. 2003. *Astrophys. J.*, 599, 363.
- Banerjee, R. & Pudritz, R. E. 2006. *Astrophys. J.*, 641, 949.
- Black, D. C., & Scott, E. H. 1982. *Astrophys. J.*, 263, 696.
- Carry, C. L. & Stahler, S. W. 2001. *Astrophys. J.*, 555, 160.
- Caselli, P., Benson, P. J., Myers, P. C., & Tafalla, M. 2002. *Astrophys. J.*, 572, 1, 238.
- Crutcher, R. M. 2012. *Annu. Rev. Astron. Astr.*, 50, 29.
- Dorfi, E. 1982. *Astron. Astrophys.*, 114, 151.
- Dudorov, A. E., & Sazonov, Yu. V. 1982. *Nauchnye Informatsii*, 50, 98.
- Dudorov, A. E., Zhilkin, A. G., & Kuznetsov, O. A. 1999. *Matem. Modelir.*, 11, 101.
- Dudorov, A. E., Zhilkin, A. G., & Kuznetsov, O. A. 1999. *Matem. Modelir.*, 11, 110.
- Dudorov, A. E., Zhilkin, A. G., Lazareva, N. Y., & Kuznetsov, O. A. 2000. *Astronomical and Astrophysical Transactions*, 19, 515.
- Dudorov, A. E., & Zhilkin, A. G. 2008. *Astron. Rep.*, 52, 790.
- Gomez, G. C., Vázquez-Semadeni, E., & Palau, A. 2021. *Mon. Not. R. Astron. Soc.*, 502, 4, 4963.
- Goodman, A. A., Benson, P. J., Fuller, G. A., & Myers, P. C. 1993. *Astrophys. J.*, 406, 528.
- Gray, W. J., McKee, C. F., & Klein, R. I. 2018. *Mon. Not. R. Astron. Soc.*, 473, 2124.
- Habe, A., Uchida, Y., Ikeuchi, S., & Pudritz, R. E. 1991. *Publ. Astron. Soc. Japan*, 43, 703.
- Hennebelle, P. & Ciardi, A. 2009. *Astron. Astrophys.*, 506, L29.
- Kargaltseva, N. S., Khaibrakhmanov, S. A., Dudorov, A. E., & Zhilkin A. G. 2021, *Bulletin of the Lebedev Physics Institute*, 48, 268.
- Khaibrakhmanov, S. A., Dudorov, A. E., Kargaltseva, N. S., & Zhilkin A. G. 2021, *Astron. Rep.*, 65, 693.
- Leao, M. R. M., de Gouveia Dal Pino, E. M., Santos-Lima, R., & Lazarian, A. 2013. *Astrophys. J.*, 777, 46.
- Li, H.-b., Dowell, C. D., Goodman, A., Hildebrand, R., & Novak, G. 2009, *Astrophys. J.*, 704, 891.
- Mouschovias, T. C. 1976. *Astrophys. J.*, 206, 753.
- Mouschovias, T. C. & Morton, S. A. 1991. *Astrophys. J.*, 371, 296.
- Myers, A. T., McKee, C. F., Cunningham, A. J., Klein, R. I., & Krumholz, M. R. 2013. *Astrophys. J.*, 766, 97.
- Nakano, T. 1979. *Publ. Astron. Soc. Japan*, 31, 697.
- Seifried, D., Pudritz, R. E., Banerjee, R., Duffin D., & Klessen, R. S. 2012. *Mon. Not. R. Astron. Soc.*, 422, 347.
- Stodólkiewicz, J. S. 1963. *Acta Astron.*, 13, 30.
- Tobin, J. J., Sheehan, P. D., Megeath, S. T., et al. 2020. *Astrophys. J.*, 890, 2, 130.
- Tomisaka, K., Ikeuchi, S., & Nakamura, T. 1988. *Astrophys. J.*, 335, 239.
- Tsukamoto, Y., Machida, M. N., Susa, H., Nomura, H., & Inutsuka, S. 2020. *Astrophys. J.*, 896, 158.
- Whitworth, A. P. & Ward-Thompson, D. 2001. *Astrophys. J.*, 547, 317.
- Zhao, B., Tomida, K., Hennebelle, P., et al. 2020. *Solar System Research*, 216, 43.
- Zhilkin, A. G., Pavlyuchenkov, Y. N., & Zamozdra, S. N. 2009. *Astron. Rep.*, 53, 590.